THE EFFECT OF PRESSURE ON THE ELECTRONIC STATES OF ORGANIC SOLIDS†

H. G. DRICKAMER

School of Chemical Sciences
and
Materials Research Laboratory
University of Illinois, Urbana, Illinois, USA

ABSTRACT

The basic effect of pressure is to decrease intermolecular distance and to increase overlap between adjacent electronic orbitals. As a consequence, there is a relative shift in energy of one type of orbital with respect to another. These shifts are particularly large for π–π^* transitions in organic molecules and for excitations in electron donor–acceptor complexes. On many occasions there are unoccupied states of sufficiently low energy such that one may obtain a new ground state at high pressure or greatly modify the characteristics of the ground state by configuration interaction. It has been shown that one can relate this thermal process to the shift of energy levels as observed by optical absorption. A number of consequences of these electronic transitions are discussed, including pressure-induced reactivity of aromatic hydrocarbons and their complexes and piezochromism in photochromic materials. Finally, it is demonstrated that one can use the shift in energy of optical absorption and emission peaks and the change in half-width of those peaks to characterize in some detail electronic excitations in a wide variety of organic molecules in the solid state and in solution.

The basic effect of pressure is to reduce intermolecular distance and thus to increase overlap between adjacent electronic orbitals. As a result, there is generally a relative shift in energy of one type of orbital with respect to another. These shifts are especially large for π–π^* excitations in aromatic hydrocarbons and related compounds and for the relatively low lying excitations in electron donor–acceptor complexes corresponding to electron transfer from donor to acceptor (from the 'no bond' to the 'electron transferred' state in Mulliken's description).

Under many circumstances there exists a second electronic state not too high in energy above the ground state. The relative shift in energy may be sufficient to give a new ground state for the system, or greatly to modify its characteristics by configuration interaction (mixing of orbitals by spin-orbit or electron-lattice coupling). These transitions may occur discontinuously at a given pressure or over a range of pressures. They occur in a wide

† This work supported in part by the US Atomic Energy Commission under Contract AT(11-1)-1198.

variety of materials with different consequences[1–3]. Electronic transitions have been observed in alkali, alkaline earth and rare earth metals with changes in electrical resistance. Insulator–metal transitions have been observed in transition metal oxides, in rare earth chalcogenides, in silicon, germanium, and a variety of III–V compounds, in molecular crystals such as iodine as well as in some crystals of large aromatic molecules. The above types of transitions are of greatest interest to the physics community.

Electronic transitions have also been observed in a wide variety of transition metal compounds, especially those of iron. These involve changes in spin state and/or oxidation state of the transition metal ion[1,2,4] and are of considerable importance in inorganic and physical chemistry as well as in geophysics.

In this paper we discuss electronic transitions in aromatic hydrocarbons and electron donor–acceptor complexes which result in enhanced chemical reactivity and in some new types of compounds, and pressure-induced transitions in photochromic bianthrones. Before taking up these specific materials we discuss some general characteristics of electronic transitions.

An electronic transition as defined above is a thermal process, i.e. it is the thermal energy of the electron which causes transfer from one orbital to another. On the other hand, the difference in energy between orbitals is normally measured by optical absorption. The thermal and optical paths differ in energy for several reasons. Two of these are illustrated in *Figure 1*. The horizontal axis is a configuration coordinate: some intermolecular (or intramolecular) displacement, such as the breathing vibration of the lattice. The vertical axis is energy. Optical excitations occur vertically (i.e. without molecular displacement) on such a diagram because they are rapid compared with molecular (or nuclear) motions, while the time scale of thermal transfer is such that a path of minimum energy may be involved. This is a major difference, but there are others of significance. In *Figure 1* the effects of configuration interaction are illustrated by the solid lines compared with the dotted line. As the lower figure indicates, an increase in configuration interaction can have different effects on the energies for the thermal and optical processes. In the third place, the optical processes are controlled by parity and other selection rules, while in the time scale of thermal processes all selection rules are relaxed. Finally, our diagram is oversimplified in that we show a single configuration coordinate, while the number of such coordinates equals the number of normal modes of the system. For thermal processes, pressure will primarily interact with a coordinate proportional

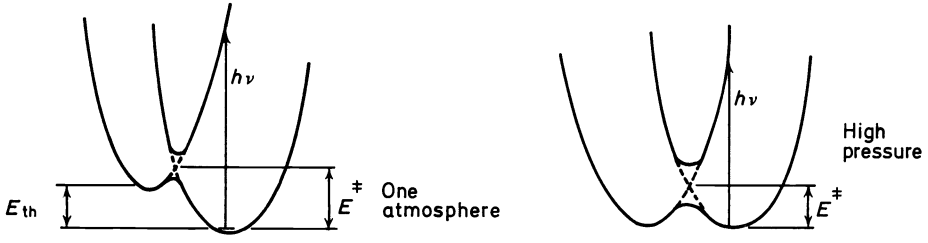

Figure 1. Schematic configuration coordinate diagram

to the volume, such as the breathing vibration of the lattice, while the optical process may involve other coordinates.

In view of all these differences the relationship between the thermal and optical processes would seem to be tenuous. However, an analysis has been performed[1,5] which relates the energies involved in optical and thermal processes. It has been quite successful in predicting electronic transitions from the location and half-width of the optical absorption peak as a function of pressure. It gives:

$$E_{th} = h\nu - 3.6(E_{1/2})^2 R \qquad (1)$$

Here E_{th} is the energy for thermal transfer, $h\nu$ is the peak location, $E_{1/2}$ the peak half-width and R the ratio of force constants of ground and excited states; all energies are in electronvolts. (We shall generally give energies in eV in this paper: 1 eV/atom $\cong$ 23 kcal/g atom $= 9.6 \times 10^4$ J/g atom. Upon occasion it will be convenient to speak of peak shifts in cm^{-1}: 1 eV $\cong$ 8000 cm^{-1}). Pressures are given in kilobars (1 kbar = 987 atm = 10^8 Pa). At the end of this paper we shall show that this analysis also forms the basis of an informative description of a wide variety of electronic excitations based on optical absorption and emission measurements as a function of pressure.

HYDROCARBONS

We consider first the electronic properties of polyacenes under pressure. We compare and contrast the behaviour of anthracene and pentacene. Both crystallize in similar 'herringbone' structures. The ground state has A_{1g} symmetry, is non-polar and is not very reactive, in the solid state at least. The lowest energy excited state wave functions have nodes between the carbons (^1L_a symmetry) and a significant dipole moment so that its interactions with neighbouring molecules must be considerably stronger than that of the ground state. Both molecules have some tendency for 'self-complexing', i.e. electron transfer between neighbours; this is greater in the excited state than in the ground state.

The major difference is that in anthracene the ^1L_a state lies over 3 eV above the ground state, while in pentacene it lies about 2 eV above the ground state. There is also a somewhat greater tendency for self-complexing for the larger molecule.

As can be seen in *Figure 2*, there is a very large decrease in optical excitation energy with increasing pressure. (A V/V_0 of 0.7 corresponds roughly to 100 kbar.) The absolute shift is about the same for both molecules, $\sim$ 0.65 eV in 100 kbar, but this constitutes a much larger fraction of the original excitation energy for pentacene than for anthracene. The peaks also broaden significantly with increasing pressure[1,5,6]. At 1 atm E_{th} for anthracene = $\sim$ 3.3 eV and for pentacene $\sim$ 2.0 eV. By 200 kbar E_{th} for anthracene is $\sim$ 1.5 eV. The rate of decrease slows rapidly with increasing pressure. The electrical resistance decreases with increasing pressure, but it always remains high and there is always a significant activation energy for carrier production, so it remains a semiconductor. All processes are reversible.

In pentacene, by 200 kbar E_{th} is $\sim$ 0. At sufficiently low temperature

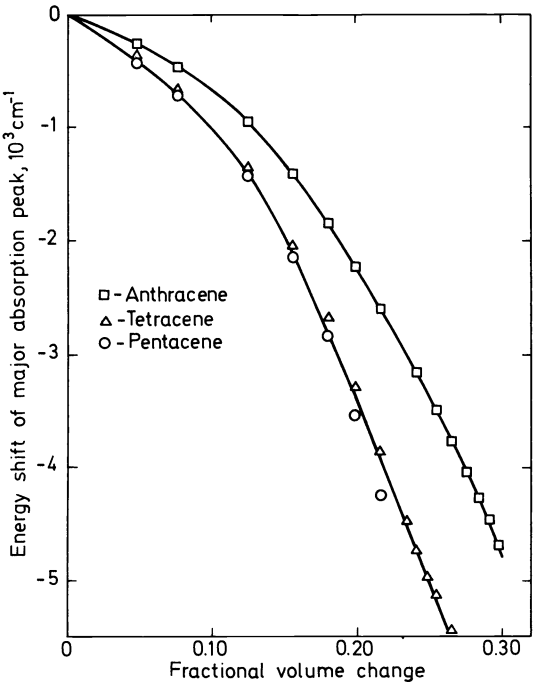

Figure 2. Shift of absorption peaks against ρ/ρ_0: three polyacenes

(below $\sim$ 200 K) one finds that the resistance increases with increasing temperature so that one has a kind of metal—probably a semimetal like bismuth with an estimated resistivity of 10^{-2}–10^{-4} ohm-cm. At room temperature above 200 kbar the resistance starts to drift upwards with time. After 24 h at 300 kbar the increase may be several orders of magnitude. This

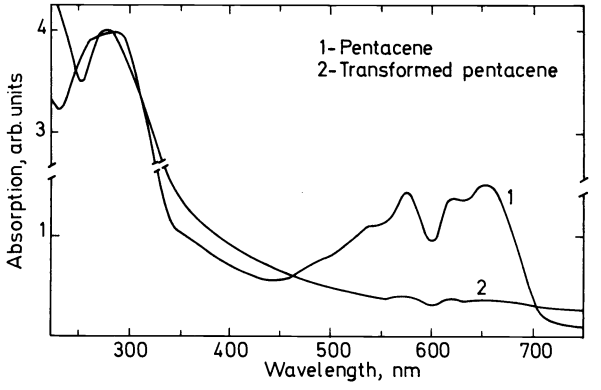

Figure 3. Electronic spectra of pentacene and reacted pentacene

is an irreversible process[1,7,8]. The material, when recovered (in milligram quantities) is reddish-brown instead of the normal bluish-black colour of ordinary pentacene. Its x-ray spectrum contains very few lines. It is non-volatile and totally insoluble in non-destructive solvents, so its characterization is difficult. One can obtain electronic and molecular spectra. The electronic spectrum appears in *Figure 3*, compared with that of ordinary pentacene. The most striking feature is the disappearance of the low-lying peaks which correspond to orbitals conjugated around the entire molecule. There are still excitations which correspond roughly to those in benzene and naphthalene.

The molecular spectrum appears in *Figure 4*. The portion between 600 and 2500 cm^{-1} is very different from that of pentacene; peaks are broadened, new peaks appear and some of the original peaks have disappeared. The most easily identifiable feature, however, is in the C—H stretching region near 3000 cm^{-1}. In pentacene there is a single peak corresponding to a typical aromatic C—H stretching frequency. In the product there is a new peak of comparable size corresponding to a typical paraffinic

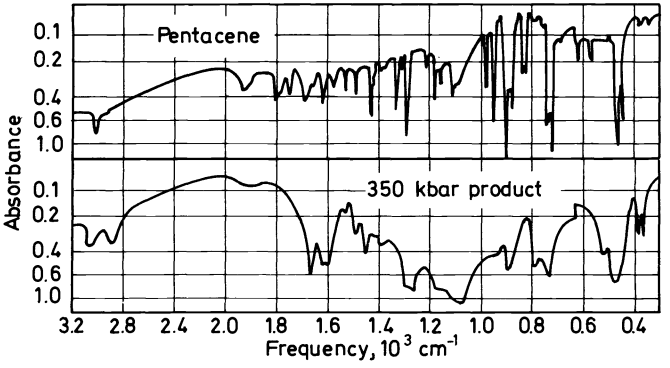

Figure 4. Infra-red spectra of pentacene and reacted pentacene

C—H frequency. Evidently the molecule has polymerized. The structure of the product is very speculative, but there must be numerous intermolecular bonds.

From the standpoint of electronic transitions, the mechanism is of interest. As illustrated in *Figure 5*, at high pressure the π orbital has increased in energy until the empty π^* orbital is available for thermal electron transfer or mixing of orbitals by configuration interaction. There may also be self-complexing between molecules in this state. This combination of events constitutes the electronic transition. Since this new state is a reactive one, the polymerization follows as a consequence of the electronic transition. Similar reactivity has been observed in a few other hydrocarbons[7,8].

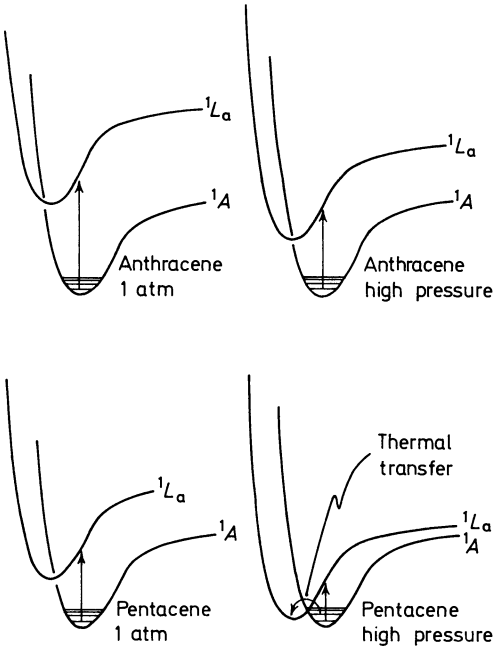

Figure 5. Configuration coordinate diagrams demonstrating the electronic transaction in pentacene

ELECTRON DONOR–ACCEPTOR COMPLEXES

A related form of chemical reactivity has been observed in a large number of electron donor–acceptor complexes. These complexes, which have been analysed in some detail by Mulliken[9], form between aromatic hydrocarbons (or related materials) as donors and such acceptors as iodine, tetracyanoethylene and halogenated hydrocarbons. The ground state is largely a 'no bond' state with a small admixture of charge transferred state, while in the excited state an electron has been transferred from the donor to the acceptor. These complexes typically have intense broad absorption peaks in the region $1\frac{1}{2}$–$2\frac{1}{2}$ eV. These peaks shift rather rapidly to lower energy with increasing pressure; a typical example is shown in *Figure 6*. They also broaden. Calculations using equation (1) indicate that for many such complexes E_{th} is reduced to zero by about 100 kbar. Some 20–30 such complexes have exhibited irreversible behaviour at high pressure as determined by electrical resistance[1,10,11]. Unfortunately, in most cases the products are complex and only modest attempts at characterization have been made.

Here we discuss two complexes where characterization of the products has been carried out to a reasonably complete degree. These are the complexes of pyrene and perylene with iodine. These complexes have a well-established stoichiometry (2 perylene $\cdot$ $3I_2$ and pyrene $\cdot$ $2I_2$) and crystal structure[12,13]. *Figure 7* illustrates the irreversible electrical behaviour. In

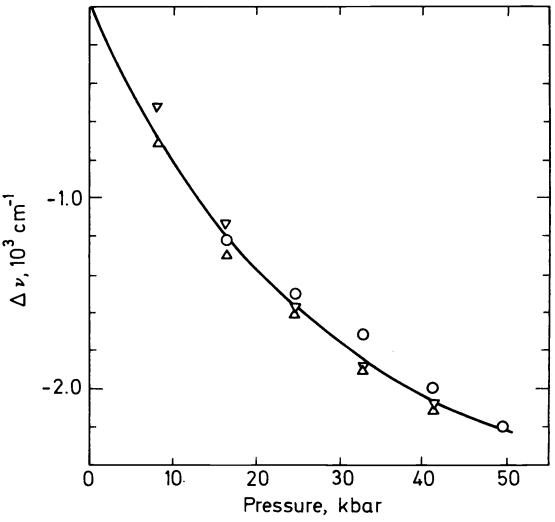

Figure 6. Shift of charge transfer peak: chloranil-hexamethyl benzene

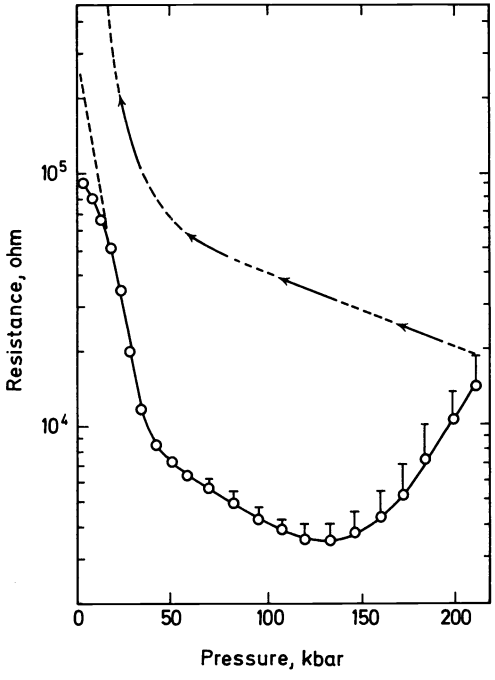

Figure 7. Resistance against pressure: pyrene · $2I_2$ complex

our apparatus only a few milligrams of material can be taken to high pressure at one load, so accumulating material for analysis is something of a tour de force. From 25–30 runs of 24 h each, at 200 kbar, a batch of 140–180 mg was accumulated. At least three such batches were produced for each complex[14].

The first point of interest is that the iodine can be quantitatively removed from the product. The presence of iodine is essential to the reaction. (The pure hydrocarbons have excited states near 3 eV and exhibit no irreversible behaviour or reactivity in this pressure range.) The function of the iodine is to provide a low-lying excited state (the electron transferred state) which can become the ground state at high pressure. Material pressed to 80 kbar and quickly released showed three times the number of unpaired spins as exhibited by the unpressed material. After 24 h at 80 kbar or after pressing to 165 kbar and quickly releasing, there were only twice the original unpaired spins, indicating that the reaction had proceeded. There were no free spins in the hydrocarbon product. This transfer of an electron to the iodine is the electronic transition. The subsequent reaction between hydrocarbons is the consequence.

Nothing is known about the structural details and interatomic distances in the material in the reactive state, or of the crystal structures of the hydrocarbon products discussed below.

The major portion of the recovered hydrocarbon is sufficiently soluble in ordinary solvents to be fractionated by chromatography. Two major fractions were recovered from the perylene product and two from the pyrene. These fractions were rather clean, but it is quite possible that each was a mixture of several closely related isomers. We shall consider each as a single compound. As established by mass spectroscopy and vapour phase osmometry, both perylene products were dimers, while both pyrene products were tetramers. The major structural determination was by n.m.r. using a Varian HR-220 with CAT attachments; molecular and electronic spectra were used to confirm some details. N.m.r. spectra run on samples from different batches and spectra obtained a month apart on a given sample yielded the same distribution of proton shifts. The arguments used to assign the structures are given in detail in the original reference. The results are summarized in *Table 1* for all four products. We mention here only the prominent features in the n.m.r. spectrum of perylene dimer A. (See *Figure 8* and *Table 1*.) It has 10 paraffinic, 2 olefinic and 3 aromatic protons. (Resonances in the range 6.8–8.0 p.p.m. downfield were assigned as aromatic, in the range 3.5–5.8 p.p.m. as olefinic and less than 3.0 p.p.m. as paraffinic.) The olefinic protons are divided into two classes. The proton appearing at 5.5 p.p.m. is approximately in its normal position, so it is not disturbed much by its environment. The proton at 3.7–3.9 p.p.m. is, however, shifted considerably upfield because of its location above the centre of an aromatic ring. Since three protons were aromatic, only one ring of the outer four in a perylene monomer had a benzenoid structure. This identifies the basic arrangement of the dimer as two skew layers with one olefinic proton positioned over a benzene ring.

The paraffinic protons appear above 3 p.p.m. In order to have 19 paraffinic protons, small rings must be involved in the crosslinking. The highest

Table 1. Structural features of products from pyrene and perylene complexes with iodine

	Pyrene tetramers		Perylene dimers	
	A	B	A	B
Number of protons	40	40	24	24
Total paraffinic protons	31	30	19	17
(a) normal ring protons	14	13	7	7
(b) three-membered ring protons at $\delta = 1.1$	5	4	4	4
(c) protons shifted downfield	12	13	8	6
Total olefinic protons	3	5	2	4
(a) at normal position	0	1	1	1
(b) shifted up field by benzene ring	3	4	1	3
No. of aromatic protons	6	5	3	3
Three-membered rings	6	5	5	4
Total aromatic rings	2	2	2	2
aromatic rings with protons	2	2	1	1
Naphthalene chromophore	0	0	1	1
Total olefin bonds	8	9	4	5
olefin bonds with protons	2	3	2	3
New bonds	18	17	11	10

field protons in dimer A are at 1.1 p.p.m. For a system with no methyl groups one would anticipate that these would be on three-membered rings. It should be noted that, in the absence of proton rearrangement, all paraffinic protons must be tertiary. Some of the protons on a three-membered ring were on carbons also involved in five-membered rings formed by the rearrangement of the original six-membered rings. These appear at 1.5 p.p.m. For dimer A, there were a minimum of four three-membered rings. Those protons appearing between 1.6 and 3.0 p.p.m. were shifted downfield by double bonds or by aromatic rings.

For details concerning the electronic and molecular spectra and the

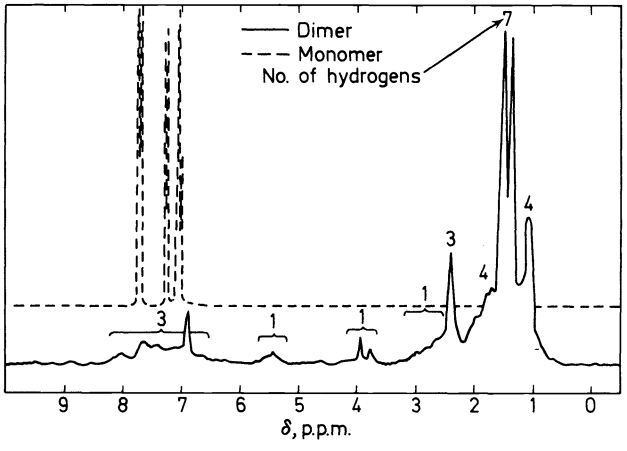

Figure 8 N.m.r. spectrum of perylene and of perylene dimer A

mass spectrum as well as a discussion of how they contribute to the structural determination the reader is referred to the original paper[14].

A model of dimer A has been developed which includes all of the characteristics listed in *Table 1*. It is shown in a stereoscopic representation in *Figure 9*

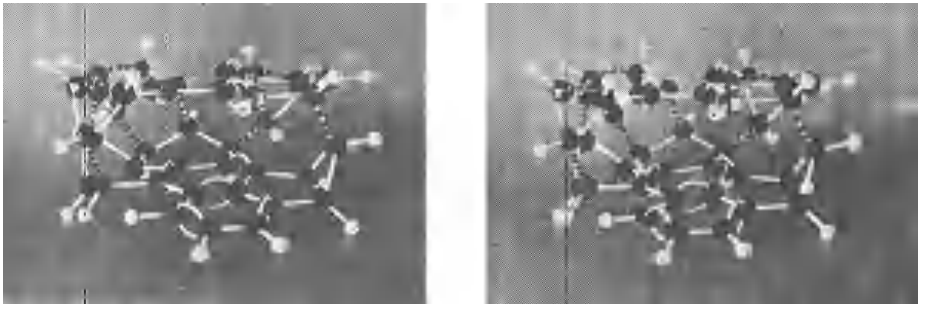

Figure 9. Stereoscopic view of perylene dimer A

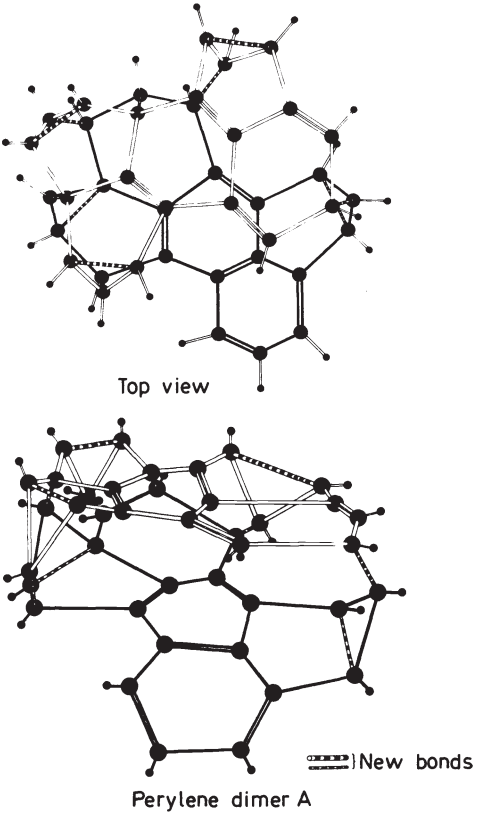

Figure 10. Front and top view of perylene dimer A

and two projections are presented in *Figure 10*. The model consists of two skew monomer layers. The molecule has five three-membered rings; the n.m.r. spectra suggest a minimum of four three-membered rings. The predicted spectrum of the model, however, agrees with the actual spectrum, since one of the protons at the tip of a three-membered ring is shifted downfield by van der Waals interaction with a nearby carbon.

The top monomer skeleton has four double bonds, which are cross-conjugated, and three cyclopropane rings. Two of the three carbons not part of double bonds or the three-membered rings are highly strained. Thus, only one carbon in the top layer of the molecule is not part of a pi system of some type. This layer is believed to be the chromophore responsible for the low-energy π–π^* absorption.

The other monomer skeleton contains the naphthalene chromophore and two three-membered rings. This naphthalene chromophore is fully conjugated to only one of the three-membered rings. There are 11 new bonds in this model of dimer A. (These appear striped in the figures.) Five of these are part of cyclopropane rings. There are six crosslinking bonds between layers. Since there is one more double bond in dimer B, only ten new sigma bonds are formed. Four of these are involved in three-membered rings and six connect the monomer layers. This model discussed above represents the characteristics displayed by the n.m.r. spectra of dimer A, as well as the u.v. and visible spectra. It is intended as a possible structure for a member of a new class of compounds formed under high pressure. Other models have been constructed; however, the one presented here fits the observed data best. These other models are similar and may also represent molecules actually present in the mixture. Models have also been constructed representing dimer B. Both products are similar.

The same type of analysis gave structures for the pyrene tetramers. In *Figure 11* we show a stereoscopic representation for pyrene tetramer A.

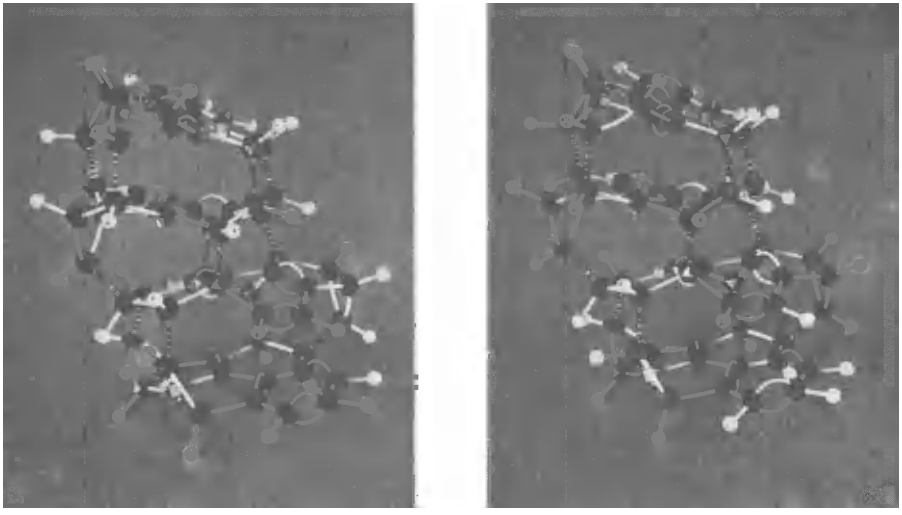

Figure 11. Stereoscopic view of pyrene tetramer A

The assignments are given in *Table 1.* It consists of four monomer-like layers turned as much as 90° out of alignment. A number of slightly different models were constructed, but this one best fits the data.

These products appear to be a new class of hydrocarbons. It is possible that one could construct electron donor–acceptor complexes with appropriate geometry and electronic structure so as to create a series of new products and to develop an organic chemistry of the solid state at high pressure.

BIANTHRONES

After optical excitation an electron may lose its energy in a number of ways. It may return to the ground state emitting fluorescent radiation or by a number of radiationless paths. It may undergo intersystem crossing to a triplet state and return to the ground state via phosphorescence or by radiationless processes. In a number of classes of molecules it may decay by one mechanism or another to a metastable state where it may remain for seconds or hours. This state will, in general, have a different (lower) excitation energy, so the material changes colour. This phenomenon is known as photochromism[15]. In organic materials the transformation to the meta-

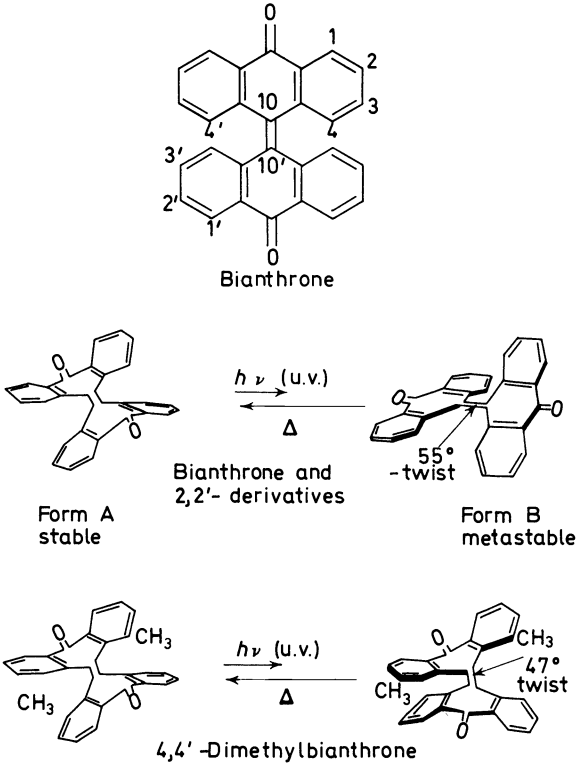

Figure 12. Structure and photochromic reactions of bianthrones

stable state involves some sort of rearrangement such as a *cis–trans* or keto–enol isomerization, a heterolytic cleavage, etc. Depending on the system, photochromism may occur in the solid, in solution or in a rigid medium such as a plastic[15]. We discuss here some high-pressure studies on a series of bianthrones[16]. (See top of *Figure 12*.) These include bianthrone (BA), 2,2′-dimethyl bianthrone (2,2′-DMBA), 2,2′-dibromobianthrone (2,2′-DBRBA) and 4,4′-dimethyl bianthrone (4,4′-DMBA). Most bianthrones undergo a photochromic rearrangement as illustrated in the centre of *Figure 12*[17] but the 4,4′-derivative, because of steric effects, undergoes the rearrangement shown at the bottom. We refer to the normal state as A and the photochromic state as B.

Bianthrones exhibit photochromism at temperatures below $\sim -50°C$ in liquid solution or in a plastic. At sufficiently elevated temperature they transform thermochromically in the liquid but not in the plastic. The crystal is neither photochromic nor thermochromic, but will transform under strong shearing action. All of these processes are reversible over a period of time.

The effects of pressure on the electronic energy levels of the four bianthrone derivatives dissolved in polymethyl methacrylate (PMMA) have been studied[16]. BA has also been studied in polystyrene (PS). All effects discussed are reversible. In *Figure 13* we exhibit the spectra of 4,4′-DMBA in its normal state and after several hours irradiation in the A peak. The

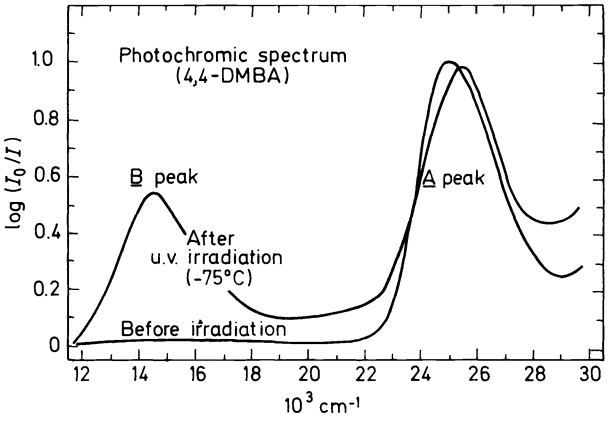

Figure 13. Spectra of unirradiated and irradiated 4,4′-DMBA in PMMA

photochromic peak (B) is obvious. In *Figure 14* we show the spectra of bianthrone (BA) at a series of pressures. The peak (B) grows with increasing pressure. Repeated spectra at the same pressure gave the same fractional conversion, so this is not an artifact of irradiation while taking the spectrum. It can also be shown that it is not a result of heating by compression. The extinction coefficients of the two peaks are roughly the same, so the relative peak areas are a reasonable measure of the fractional conversion. The fraction converted is shown as a function of pressure in *Figure 15* for BA.

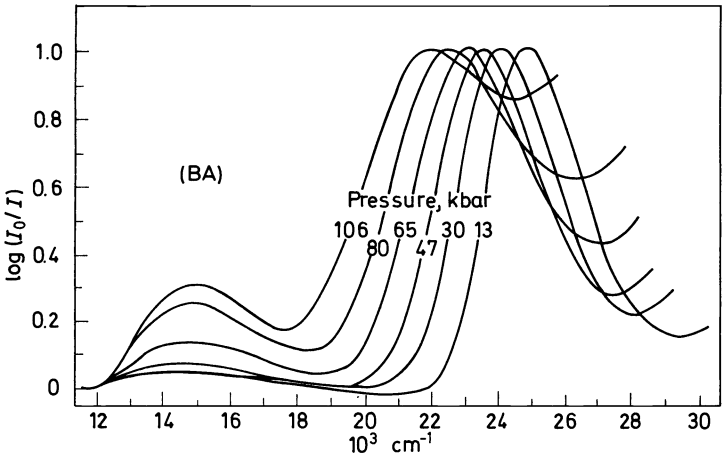

Figure 14. Spectra of BA in PMMA at various pressures

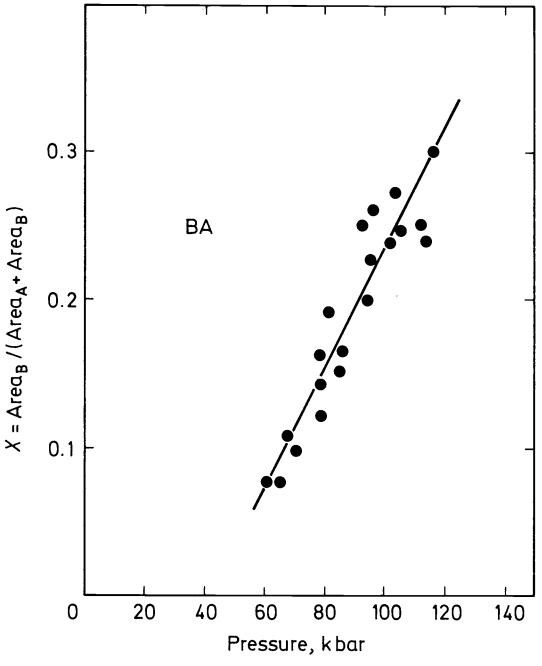

Figure 15. Conversion from A to B form against pressure: BA in PMMA

Other derivatives gave different conversions; the 4,4'-DMBA showed an especially small yield. The amount of product formed varied also with the medium. In *Figure 16* we exhibit a simple configuration coordinate diagram where the mode involved is the reaction coordinate. In the original paper

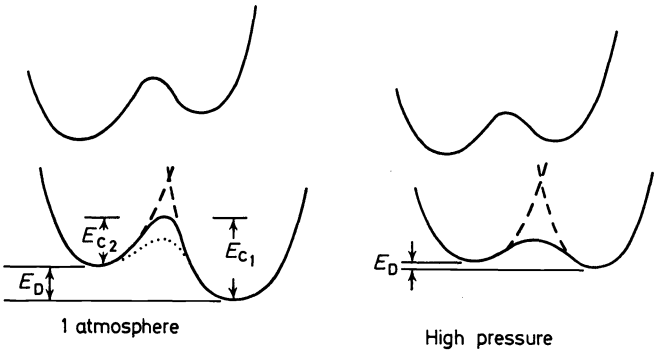

Figure 16. Configuration coordinate diagram for conversion between A and B forms

calculations using equation (1) demonstrate that the thermal process is directly from the A ground state to the B ground state to the B ground state; i.e. no thermal occupation of the excited A state is involved. In the steady state

$$(1 - x)\exp(-E_{c_1}/kT) = x\exp(-E_{c_2}/kT) \tag{2}$$

or

$$x = 1/[1 + \exp(E_D/kT)] \tag{3}$$

where x is the fraction converted and E_{c_1}, E_{c_2} and E_D are defined in *Figure 16*. A plot of E_D/kT vs pressure for BA is shown in *Figure 17*. If equilibrium has been reached, one can calculate the increase in yield upon raising the temperature, using E_D evaluated from room temperature data. As shown in

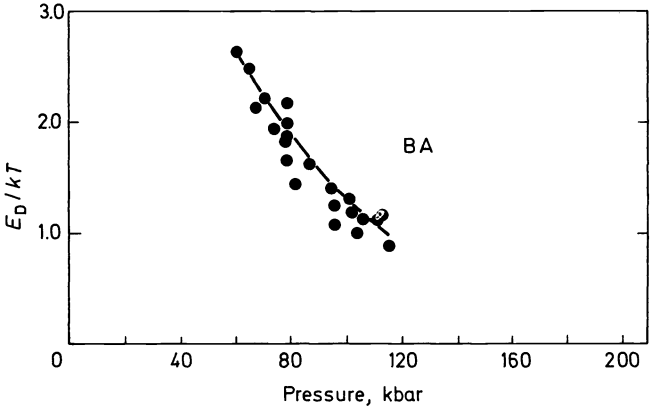

Figure 17. E_D/kT ($\Delta G_{AB}/kT$) against pressure: BA in PMMA

the original paper, equilibrium is indeed attained. One can then consider E_D as a free energy difference ΔG_{AB}, and write:

$$\partial \ln K/\partial p = -\partial \Delta G_{AB}/\partial p = -\Delta \overline{V}_{AB}/kT \qquad (4)$$

where $\Delta \overline{V}_{AB}$ is the difference in partial molar volumes between the two states. Typical values appear in *Table 2*. The volume of the B state is less than that of the A state, but its compressibility is less also, so that at sufficiently high pressure they should attain the same volume. $\Delta \overline{V}_{AB}$ for 4,4′-DMB is noticeably smaller than that for the other derivatives. This is not surpirsing in view of its different conformation, but it is of interest to have a quantitative measure.

The difference in behaviour between BA in PMMA and in PS is illustrated in *Figure 18*, where E_D/kT ($\Delta G_{AB}/kT$) is plotted against ρ/ρ_0. The plots

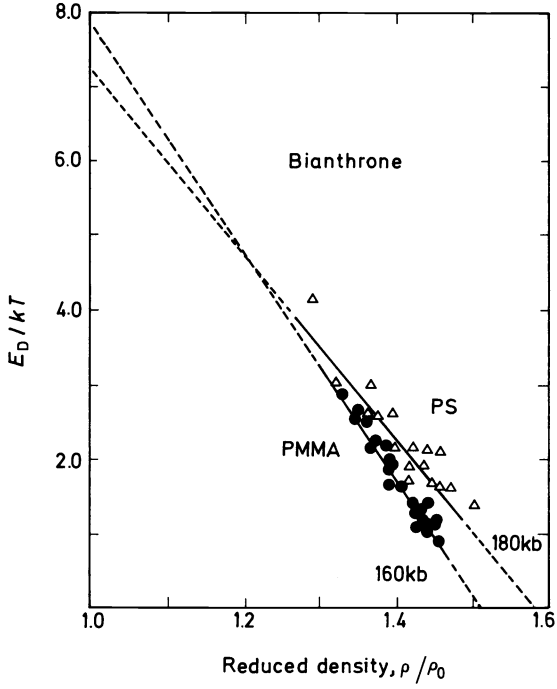

Figure 18. E_D/kT ($\Delta G_{AB}/kT$) against ρ/ρ_0: BA in PMMA and in PS

appear linear although there is considerable scatter, and the range is short, so this point should not be overemphasized.

Qualitatively one associates the decrease in E_D with increasing density with a stronger attractive interaction of the B state with the medium than that for the A state. This could be associated with a larger dipole moment and/or polarizability for the A state. While either state apparently has a permanent dipole moment, the electronic states of the two forms apparently differ enough to allow quite different polarizabilities. It may be relevant

Table 2. $\Delta\bar{V}_{AB}$ for bianthrones

Compound	ΔV_{AB}, cm³/mol Pressure, kbar 60	90	120
BA in PMMA	−0.9	− 0.7	− 0.5
2,2′-DMBA in PMMA	− 1.1	− 0.7	− 0.3
2,2′-DRBA in PMMA	− 0.9	− 0.8	− 0.7
4,4′-DMBA in PMMA		− 0.4	
BA in PS	− 0.8	− 0.3	

to point out that for xanthylidenanthrone, which undergoes a similar transformation, the molar polarizations of the B and A forms have the ratio $P_B/P_A = 2.3$[18]. The smaller decrease in E_D with density in PS compared with PMMA may be associated with its smaller dielectric constant ($\varepsilon_{PS} = 2.6$ and $\varepsilon_{PMMA} = 3.5$), and thus with a weaker solute–solvent interaction.

This is, then, a pressure-induced electronic transition of a type which can only be produced by light or heat under ordinary pressures. There is preliminary evidence that similar transitions occur at high pressure in some spiropyrans and perhaps in some stilbenes also.

ANALYSIS OF CONFIGURATION COORDINATE PARAMETERS

The configuration coordinate analysis discussed at the beginning of this paper can be used as a basis for characterizing a wide variety of electronic excitations. In the course of its derivation, equations were developed for the shift of the optical absorption (or emission) peak with pressure and the change of half-width. These can conveniently be written:

$$(\delta h\nu)_a = pR\Delta + p^2\frac{(R-1)}{2\omega^2} + \frac{R^2\Delta^2}{2}(\omega^2 - \omega_0^2) \tag{5}$$

$$(\delta h\nu)_e = \frac{p\Delta}{R} + \frac{p^2(R-1)}{2\omega^2R^2} - \frac{\Delta^2}{2}(\omega^2 - \omega_0^2) \tag{6}$$

$$\delta(E_{1/2})_a = N\left[\left|\omega R\Delta + \frac{p(R-1)}{\omega}\right| - \left|\omega_0 R\Delta\right|\right] \tag{7}$$

$$\delta(E_{1/2})_e = N\left[\left|\frac{\omega\Delta}{R^{1/2}} + \frac{p(R-1)}{\omega R^{3/2}}\right| - \left|\frac{\omega_0\Delta}{R^{1/2}}\right|\right] \tag{8}$$

Here $h\nu$ represents the energy of the peak maximum, $E_{1/2}$ the peak width at half height and δ the change in the value of the quantity between pressure p and 1 atm (effectively zero pressure). Δ, the displacement along the configuration coordinate of the excited state potential well with respect to the ground state well, could be considered as the change in volume of the system upon excitation of an electron, at least if the normal mode in question is the breathing vibration of the system. The potential wells are considered as harmonic with force constants ω^2 and ω'^2. $R = (\omega'/\omega)^2$, and $N = (8kT\ln 2)^{1/2}$ for Gaussian peaks at ordinary temperatures. ω^2 is considered to be pressure dependent, and ω_0^2 is the value at 1 atm. It is assumed that R is constant or at least varies slowly with pressure compared with ω^2. This

seems reasonable and no available data justify a more complex pressure dependence.

In general, the shift of the optical absorption or emission peak with pressure can be expressed within the accuracy of most data as a quadratic function of pressure. The change of half-width may be linear or quadratic in pressure. This gives six or eight measured coefficients to determine R, Δ, and the pressure dependence of ω^2. (For some systems ω^2 may be independent of pressure; for others, a reasonable assumption may be that it is coupled to the bulk modulus of the crystal or solvent, e.g. in the form $\omega^2 = \beta(-\partial p/\partial V)$, which defines a dimensionless β.) In any case, the three parameters are considerably overdetermined if accurate peak shift and half-width change data are available for both absorption and emission. This gives the opportunity to calculate them from several combinations of the coefficients, and provides a test of the consistency of the data and the applicability of the configuration coordinate model. It is, of course, necessary that the emission occur from the same state as that to which the electron is excited, with no intersystem crossing. Otherwise, additional parameters are needed and the redundancy may disappear. Problems in measurement and calculation of half-widths under pressure have been discussed in some detail elsewhere[19].

As indicated above, one would use various combinations of absorption and fluorescence data to calculate Δ, R and the pressure dependence of ω^2. Four such methods used in this laboratory include:

(1) A method based on absorption data only, using the linear and quadratic coefficients from fitting the peak shift data and a linear term from the change of half-width with pressure.

(2) A similar calculation using emission data only.

(3) A combination of absorption and emission data, using the linear coefficients for peak shift of the absorption and emission peaks and the change of half-width of (say) the absorption peak. This method emphasizes the low-pressure data.

(4) A calculation using only the shifts of absorption and emission peaks which does not involve any half-width data.

Table 3. Configuration coordinate parameters for phenanthrene crystal

Method	Δ	R	β
1	3.7	1.01	1.4
2	− 3.8	0.99	1.7
3	− 3.8	1.00	1.3
4	− 3.8	1.01	1.6

This analysis has been applied successfully to a number of systems[20,21]. We discuss only a representative set of data here. In *Table 3* we exhibit results for phenanthrene in the crystal. The agreement among the methods is very good, which lends considerable credence to the analysis.

In *Table 4* we compare values for the configuration coordinate parameters

Table 4. Configuration coordinate parameters

Material	Δ(cm^3/mol)	R	β
Phenanthrene			
in crystal	− 3.7	1.01	1.4
in PMMA	− 1.0	1.00	0.53
in hexane	− 3.1	1.00	0.016
Anthracene			
in crystal	− 10.2	1.00	1.1
in PMMA	− 3.3	1.01	0.27
in hexane	− 9.2	1.00	1.7×10^{-3}
in methanol	− 7.4	1.00	2.9×10^{-3}
in glycerol	− 5.7	1.02	0.18

Δ, β and R for phenanthrene and anthracene in various media. The decrease in volume of the system upon electronic excitation, Δ, depends strongly on the medium. There is a balance among several factors: the increase in dipole moment of the molecule upon electronic excitation, the polarizability of the surrounding medium and the compressibility of the medium. The crystal has a larger polarizability than the PMMA or the hexane, while the hexane has a much larger compressibility than the crystal of PMMA. The balance of these factors gives the resultant value of Δ. The effect of compressibility can be seen in the data for anthracene in hexane, methanol and glycerol. The relative compressions of the solvents in 10 kbar are 0.31/0.25/0.12. The excited state of anthracene (^1L_a) has a much larger dipole moment than the excited state of phenanthrene (^1L_b). The ratio of the Δ values for the two molecules are: in the crystal 2.7, in PMMA 3.3, and in hexane 3.2.

β is largest for the most rigid medium, the crystal; smaller by a factor of three for PMMA; and smaller by two orders of magnitude in hexane. For anthracene the βs are in the ratio 1/1.7/100 for hexane/methanol/glycerol. The viscosities of the three solvents are in the ratio 1/1.7/1200. There is a clear relationship between the stiffness of the medium and the coupling to the solute molecule.

For these and other π–π^* excitations $R \simeq 1.0$. This is not necessarily general. For impurities in alkal halides values of R ranging from 0.5 to 1.5 have been observed.

In addition to studies on aromatic hydrocarbons in various environments[20], this analysis has been successfully applied to purine and pyrimidine bases and the corresponding nucleosides in the crystal, in neutral aqueous solution and in acidic and basic solution[21]. It appears to be a powerful method for characterizing electronic excitations.

ACKNOWLEDGEMENT

The author is indebted to many students for contributions to all aspects of this work; to Professor C. P. Slichter for his essential collaboration in the configuration coordinate analysis; and to Professors J. C. Martin, N. J. Leonard and S. G. Smith for vital assistance in unravelling the structure of the perylene dimers and the pyrene tetramers. The support of the US Atomic Energy Commission in this research is gratefully acknowledged.

REFERENCES

[1] H. G. Drickamer and C. W. Frank, *Electronic Transitions and the High Pressure Chemistry and Physics of Solids*. Chapman and Hall: London; Halsted Press: New York (1973).
[2] H. G. Drickamer and C. W. Frank, *Ann. Rev. Phys. Chem.* **23**, 39 (1972).
[3] H. G. Drickamer, *Chem. Brit.* **9**, 353 (1973).
[4] H. G. Drickamer, *Angew. Chem.* **13**, 39 (1974).
[5] H. G. Drickamer, C. W. Frank and C. P. Slichter, *Proc. Nat. Acad. Sci. Wash.* **69**, 933 (1972).
[6] G. A. Samara and H. G. Drickamer, *J. Chem. Phys.* **37**, 474 (1962).
[7] R. B. Aust, W. H. Bentley and H. G. Drickamer, *J. Chem. Phys.* **41**, 1856 (1964).
[8] V. C. Bastron and H. G. Drickamer, *J. Solid State Chem.* **3**, 550 (1971).
[9] R. S. Mulliken and W. B. Person, *Molecular Complexes*. Wiley-Interscience: New York (1969).
[10] W. H. Bentley and H. G. Drickamer, *J. Chem. Phys.* **42**, 1573 (1965).
[11] R. B. Aust, G. A. Samara and H. G. Drickamer, *J. Chem. Phys.* **41**, 2003 (1964).
[12] T. Uchida and H. Akamata, *Bull. Chem. Soc. Japan*, **34**, 1015 (1961).
[13] O. Hassel and C. Romming, *Quart. Rev.* **16**, 1 (1962).
[14] M. I. Kuhlman and H. G. Drickamer, *J. Amer. Chem. Soc.* **94**, 8325 (1972).
[15] G. H. Brown (ed.), *Photochromism*. Wiley-Interscience: New York (1971).
[16] D. L. Fanselow and H. G. Drickamer, *J. Chem. Phys.* **61**, 4567 (1974).
[17] R. Korenstein, K. A. Muszkat and S. Sharafy-Ozeri, *J. Amer. Chem. Soc.* **95**, 6177 (1973).
[18] Y. Hirschberg and E. Fischer, *J. Chem. Phys.* **23**, 1723 (1955).
[19] B. Y. Okamoto, W. D. Drotning and H. G. Drickamer, *Proc. Nat. Acad. Sci., Wash.* **71**, 2621 (1974).
[20] B. Y. Okamoto and H. G. Drickamer, *J. Chem. Phys.* **61**, 2870 (1974).
[21] B. Y. Okamoto and H. G. Drickamer, *J. Chem. Phys.* **61**, 2878 (1974).

APPENDIX

The theme of this paper is the effect of pressure on electronic energy levels in solids, and resulting chemical reactivity. However, there is also a very extensive area of research involving the effect of pressure on chemical reactivity in solution. This has generally been limited to pressures in the range of 5–10 kbar, but since organic liquids compress 16–20 per cent in 5 kbar and 25–30 per cent in 10 kbar, significant results can be expected. These studies fall into two general areas: the inducing of new chemical reactions or the enhancement of yield in chemical reactions, and studies of the effect of pressure on reaction rate in order to elucidate the mechanisms of reactions. A general review of the area is given by Weale[1A]. Important contributions for both organic and inorganic systems have been made by Osugi and co-workers[2A–6A]. A recent paper by Dauben and Kozikowski[7A] is a particularly nice example of the use of pressure to overcome stereochemical resistance to reaction.

Physical-organic chemistry at high pressure has been reviewed by LeNoble[8A] and by Eckert[9A], both of whom have made important contributions. Johnson, Eyring and Stover[10A] discuss pressure effects on rate processes in biological systems.

The basic approach to physical-organic chemistry in this area is to start from an equation for the reaction velocity constant:

$$k = (k_B T/h) \exp(-\Delta G^{+}/RT) \tag{A1}$$

where k_B is Boltzmann's constant, h is Planck's constant, T the temperature

and ΔV^{+} the 'free energy of activation', i.e. the difference between the free energy in the transition state and that of the reactants.
Then:

$$(\partial \ln k/\partial p)_T = -\Delta V^{+})/RT = (V_r - V^{+})/RT \qquad \text{(A2)}$$

Thus, from the pressure coefficient of the reaction velocity constant one can calculate the volume change between reactants and transition state. This is often very helpful in deciding between various reaction mechanisms and in formulating a picture of reaction dynamics.

In addition to the above comments on reaction in solution, it is appropriate to add a remark vis á vis the main theme of the paper. There has been a recent significant study[11A] of the effect of pressure to several hundred kilobars on reactivity of some aromatic diamine–chloranil complexes. In some cases the products could be reasonably identified.

REFERENCES TO APPENDIX

[1A] K. A. Weale, *Chemical Reactions at High Pressure.* Spon: London (1967).
[2A] J. Osugi and K. Hara, *J. Chem. Soc. Japan*, **92**, 601, 608 (1971).
[3A] J. Osugi, *Rev. Phys. Chem. Japan*, **40**, 122 (1971).
[4A] K. Hara and J. Osugi, *Chemistry*, **28**, 62 (1973).
[5A] J. Osugi, *Bull. Inst. Chem. Res. Kyoto Univ.* **47**, 96 (1974).
[6A] J. Osugi and I. Oniski, *J. Chem. Soc. Japan*, **92**, 702 (1972).
[7A] W. G. Dauben and A. P. Kozikowski, *J. Amer. Chem. Soc.* **96**, 3664 (1974).
[8A] W. J. LeNoble, *J. Chem. Educ.* **44**, 729 (1967).
[9A] C. A. Eckert, *Ann. Rev. Phys. Chem.* **23**, 239 (1972).
[10A] F. H. Johnson, H. Eyring and B. J. Stover, *The Theory of Rate Processes in Biology and Medicine.* Wiley-Interscience: New York (1974).
[11A] T. Sakata, A. Onodera, H. Tsubomura and N. Kawai, *J. Amer. Chem. Soc.* **96**, 3365 (1974).